Publishing House
AKAPIT

COMPUTER METHODS IN MATERIALS SCIENCE

Informatyka w Technologii Materiałów

Vol. 8, 2008, No. 3

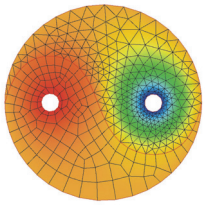

RECTILINEAR VISCOELASTIC FLOWS IN DUCTS

MICHEL BEAULNE[1], EVAN MITSOULIS[2*]

[1] Department of Chemical Engineering, University of Ottawa, Ottawa, Ontario, K1N 6N5, Canada
[2] School of Mining Engineering and Metallurgy,
National Technical University of Athens, Zografou 157 80, Athens, Greece
Corresponding author: mitsouli@metal.ntua.gr (E. Mitsoulis)

Abstract

Axial flows in generalized ducts are studied for viscoelastic materials including a linear low-density polyethylene (LLDPE) melt. Viscoelasticity is described by an integral constitutive equation of the K-BKZ type with a spectrum of relaxation times, which fits well experimental data for the shear and elongational viscosities and the normal stresses as measured in shear flow. The K-BKZ model can be reduced to the Newtonian and Maxwell models with appropriate choice of the parameters. A new technique is developed where the Finger and Cauchy-Green tensors are simplified for axial flows, since particle tracking is only required in the flow z-direction (not required in the x-y coordinate plane). Numerical solutions are presented in two-dimensional cross-sectional geometries, namely square, concave square, and eccentric annulus, for different flow rate and pressure drop changes. For the Maxwell model, the dimensionless pressure drop is independent of the Weissenberg number and a function only of the geometry. For the K-BKZ model representing the LLDPE melt, the dimensionless pressure drop is reduced with increasing flow rate, hence Weissenberg number. The present results are offered as benchmark solutions for the imposition of entry velocity and stress profiles in three-dimensional ducts, when secondary flows are not present.

Key words: Viscoelasticity, K-BKZ constitutive equation, Maxwell model, Ducts, LLDPE melt

1. INTRODUCTION

Materials processing (including polymer processing) involves flows in ducts of both simple and complex shape. In numerical simulations, it is necessary to impose entry boundary conditions in such geometries of arbitrary shape, by satisfying the flow rate vs. pressure drop condition for a given duct area. Thus, the equations of conservation for mass and momentum are solved to determine the velocity and stress profiles of the entering material in the duct. In general, this corresponds to a three-dimensional (3-D) problem, with all 3 velocity components present. The usual procedure is the solution of a 2½-D problem, where the 3 velocity components are only functions of (x,y). This was the approach adopted by Dupont & Crochet (1987), Gervang & Larsen (1991), Xue et al. (1995), Debbaut et al. (1997). Then secondary effects are obtained when a second normal-stress difference is present. However, the problem is involved and nontrivial.

Another approach adopted here is the solution of a two-dimensional (2-D) problem by assuming no second normal-stress difference, hence no secondary flows, but simple rectilinear flows. Then the resulting equation is the Poisson equation for the axial velocity in a generalized 2-D domain with the pressure gradient as the source term.

For this type of problem the solutions for the Newtonian, pseudoplastic (power-law), and viscoplastic (Bingham) fluids for generalized ducts have already been determined (see, e.g., Middleman,

ISSN 1641-8581

1965; Huilgol & Panizza, 1995; Taylor & Wilson, 1997; Pham & Mitsoulis, 1998). Wachs et al. (1999) have simulated axial flows of viscoelastic fluids in square ducts by mapping the region of flow into a circular domain. The constitutive equation used by Wachs et al. (1999) was the K-BKZ integral constitutive equation.

In the present paper, we extend the work of Pham & Mitsoulis (1998) carried out for viscoplastic Bingham materials, and study the flow of viscoelastic fluids. The solutions for viscoelastic materials for generalized ducts are here determined for three cross-sectional areas (square, concave, eccentric annulus) for the Newtonian, integral upper-convected Maxwell (UCM), and integral K-BKZ constitutive equations. For the case of the K-BKZ equation, an LLDPE melt is used, as described by Guillet at al. (1996). Contours for the velocity and the magnitude of the stress tensor are given for the LLDPE melt for different geometries. The emphasis is based on using appropriate dimensionless variables to present the simulation results. In this form, they can be used by engineers for quick calculations, in cases where viscoelastic materials flow through ducts of arbitrary shape, as is the case in extrusion die flow.

2. MATHEMATICAL MODELLING

The flows considered here are steady, rectilinear (no secondary flows present), unidirectional (axial) flows through ducts of generalized shape, e.g., square and concave rectangular, and eccentric annuli. These are common cross-sections of extrusion dies (Walton & Bittleston, 1991). They are used here for their simplicity and for deriving benchmark solutions for the open literature. A schematic representation of the domain of interest and the boundary conditions involved are given in figure 1. For axial rectilinear flows, the flow is unidirectional (z-direction only), and transverse circulation is negligible (Tanner, 2000). The flow is governed by the usual conservation equations of mass and momentum, i.e.

$$\bar{\nabla}\,\bar{v} = 0\,, \tag{1}$$

$$0 = -\bar{\nabla}p + \bar{\bar{\nabla}}\bar{\bar{\tau}}\,, \tag{2}$$

where $\bar{v}$ is the velocity vector, p is the scalar pressure, and $\bar{\bar{\tau}}$ is the extra stress tensor. For axial flows, these equations are simplified to give the expression for the flow rate and the Poisson equation with the pressure gradient as the source term:

$$Q = \iint_A v_z(x,y)\,dxdy \tag{3}$$

$$\frac{\partial \tau_{zx}}{\partial x} + \frac{\partial \tau_{zy}}{\partial y} = \frac{dP}{dz} \tag{4}$$

These equations describe flow due to a constant pressure gradient dP/dz in the z-direction, through a duct extending in the x- and y-directions with zero velocity along its perimeter (no-slip condition, see figure 1).

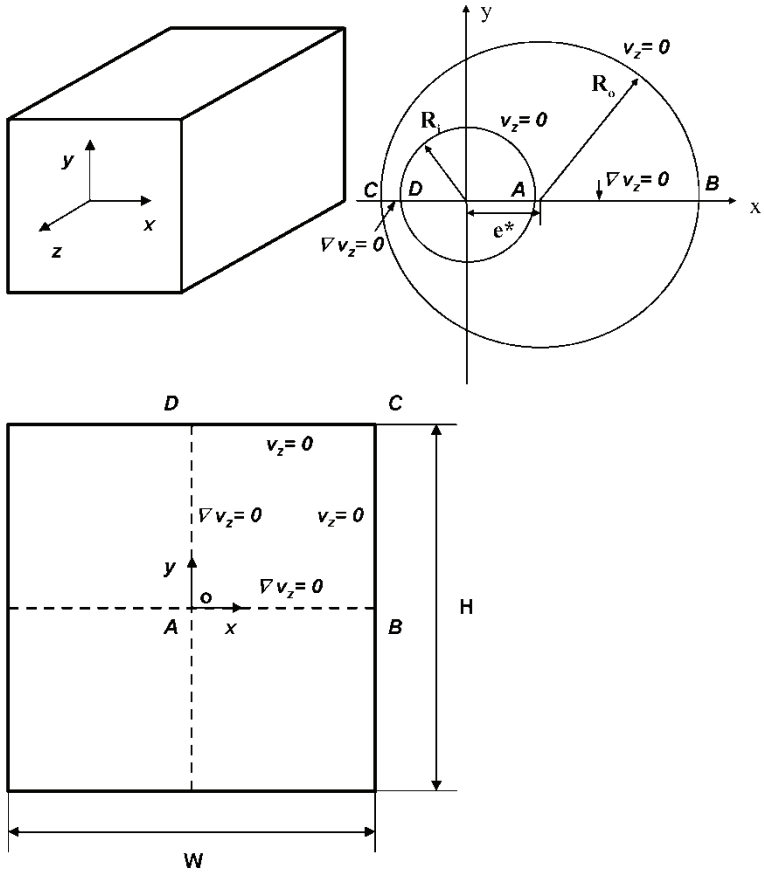

Fig. 1. *Schematic representation of flow through a cross-section of a square and an annular duct along with relevant notation and boundary conditions.*

The constitutive equation that relates the stresses τ to the deformation history is an integral model of the K-BKZ type proposed by Papanastasiou et al. (1983) and further modified by Luo & Tanner (1988). It is written as

$$\overline{\overline{\tau}}(t)=\frac{1}{1-\theta}\int_{-\infty}^{t}\sum_{k=1}^{N}\frac{a_k}{\lambda_k}\exp\left(-\frac{t-t'}{\lambda_k}\right)\frac{\alpha_k}{(\alpha_k-3)+\beta_k I_{C^{-1}}+(1-\beta_k)II_{C^{-1}}}\times\left[\left\{\overline{\overline{C}}_t^{-1}(t')\right\}+\theta\left\{\overline{\overline{C}}_t(t')\right\}\right]dt' \quad (5)$$

where λ_k and a_k are relaxation times and relaxation modulus coefficients, respectively, for N relaxation modes. The parameters α_k and β_k are material parameters chosen to fit the material's response in strong shear and elongation. The parameters $I_{C^{-1}}$ and $II_{C^{-1}}$ are the first and second invariants of the Finger strain tensor $\overline{\overline{C}}_t^{-1}$. The second invariant $II_{C^{-1}}$ is equal to the first invariant I_C of the Cauchy-Green tensor $\overline{\overline{C}}_t$. The parameter θ has been incorporated by Luo & Tanner (1988) to take into account the second normal stress difference, N_2, and is related to the first normal stress difference, N_1, via the formula

$$\frac{N_2}{N_1}=\frac{\theta}{1-\theta}. \quad (6)$$

The value of θ is non-zero for polymer melts exhibiting a second normal stress difference. Its usual range is between 0 and –0.3 (Tanner, 2000). It is this non-zero value that is responsible for secondary flows in ducts. Therefore, for the present work it is essential that θ is set to 0.

The modified K-BKZ model reduces to the Newtonian model when N=1 and λ_1=0 or respectively a small number, say λ_1=0.001. The K-BKZ model also reduces to the integral upper-convected Maxwell (UCM) model when N=1 and $\alpha\to+\infty$, or say a large number $\alpha=10{,}000$.

In terms of the deformation gradient tensor, $\overline{\overline{F}}_t(t')=d\overline{\boldsymbol{x}}'/d\overline{\boldsymbol{x}}$, the Cauchy-Green and Finger strain tensors are

$$\overline{\overline{C}}_t(t')=\overline{\overline{F}}_t(t')\left[\overline{\overline{F}}_t(t')\right]^T$$
$$\overline{\overline{C}}_t^{-1}(t')=\left[\overline{\overline{F}}_t^{-1}(t')\right]^T\overline{\overline{F}}_t^{-1}(t') \quad (7)$$

The Finger and Cauchy-Green tensors are found analytically since the domain is considered infinitely long in the z-direction. The assumption is also made that transverse circulation is negligible (Tanner, 2000). For axial flows, the Finger and Cauchy-Green tensors are determined as

$$\overline{\overline{C}}_t(t')=\begin{bmatrix}1 & 0 & -\frac{dw}{dx}(t-t')\\ 0 & 1 & -\frac{dw}{dy}(t-t')\\ -\frac{dw}{dx}(t-t') & -\frac{dw}{dy}(t-t') & 1+\left[\frac{dw}{dx}(t-t')\right]^2+\left[\frac{dw}{dy}(t-t')\right]^2\end{bmatrix} \quad (8)$$

$$\overline{\overline{C}}_t^{-1}(t')=\left[\overline{\overline{C}}_t(t')\right]^{-1} \quad (9)$$

where $w=v_z(x,y)$ is the velocity in the positive z-direction (see figure 1) and $(t-t')$ represents the time lapse between a time in the past t' and the present time t.

The viscoelastic character of the flow is assessed by a dimensionless number known as the Weissenberg number, and is defined as

$$Ws=\bar{\lambda}\,\bar{\dot{\gamma}} \quad (10)$$

Here, $\bar{\lambda}$ is the average relaxation time given by:

$$\bar{\lambda}=\frac{\sum_{k=1}^{N}\lambda_k^2\,a_k}{\sum_{k=1}^{N}\lambda_k\,a_k} \quad (11)$$

and $\bar{\dot{\gamma}}$ is the average shear rate given by

$$\bar{\dot{\gamma}}=\bar{v}/R_h \quad (12)$$

In the above, R_h is the hydraulic radius defined as the cross-sectional area A of the duct divided by its perimeter Π, $\bar{v}$ is the average velocity of the viscoelastic material in the duct, given by the volumetric flow rate Q divided by the area, A. A dimensionless pressure gradient can also be defined as the Hagen number

$$Ha=\frac{\left(\frac{dP}{dz}\right)(2R_h)^2}{\mu\bar{v}_N} \quad (13)$$

where $\bar{v}_N$ is the average velocity of an equivalent Newtonian fluid with viscosity μ.

3. RHEOLOGICAL CHARACTERIZATION

For the case of a typical polymer melt able to be described rheologically by the K-BKZ model, we have chosen an LLDPE melt with data given by Guillet et al. (1996). They measured the shear viscosity, first normal stress difference, and uniaxial extensional viscosity under varying shear and elongational rates. Also measured was the storage and loss modulus at varying frequencies. The relaxation spectrum used here is the same as that determined by Guillet et al. (1996) for the Wagner model. The parameters α and β were chosen to best fit the material's response in strong shear and elongation. No second normal-stress difference data are given for this LLDPE melt, but it is usually assumed to be negligible. Therefore in the simulations we have used a zero second normal-stress difference (θ=0 in Eq. 5). The values for the relaxation spectrum and associated constants from the K-BKZ integral equation for the LLDPE melt are given in Table 1. With these values, the predictions for the shear viscosity η_S as a function of the shear rate $\dot{\gamma}$, the elongational viscosity η_E as a function of the elongational rate $\dot{\varepsilon}$, and the first normal stress difference N_1 as a function of shear rate $\dot{\gamma}$, are plotted in figure 2, together with the experimental data. As well, the predictions for the storage modulus G' and loss modulus G'' as a function of frequency ω, are plotted in figure 3, together with the experimental data. It should be noted that the flows studied here are *shear* flows, and therefore the extensional data are only used for the completion of the model.

Table 1. *Material parameter values used in Eq. (5) for fitting data for the LLDPE at 160°C according to Guillet et al. (1996)* ($\alpha = 5.0$, $\beta = 0.041$, $\theta = 0$)

k	λ_k (s)	a_k (Pa)
1	1.28×10^{-4}	1.85×10^{6}
2	6.12×10^{-3}	2.20×10^{5}
3	4.10×10^{-2}	8.20×10^{4}
4	2.77×10^{-1}	1.69×10^{4}
5	2.01×10^{0}	1.85×10^{3}
6	1.57×10^{1}	1.28×10^{2}
7	1.35×10^{2}	7.08×10^{0}

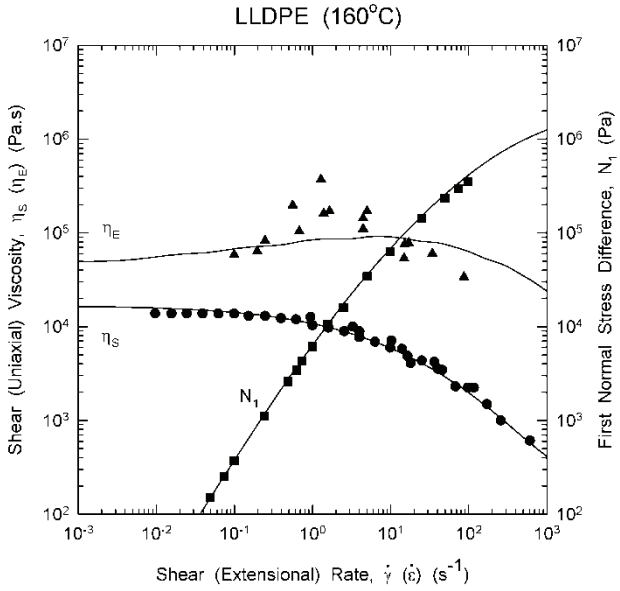

Fig. 2. *Model predictions of shear viscosity η_S and first normal stress difference N_1 vs. shear rate $\dot{\gamma}$, and elongational viscosity η_E vs. elongational rate $\dot{\varepsilon}$ for the LLDPE melt at 160°C using Eq. (5) with the material parameters given in Table 1. Symbols are experimental data reported by Guillet et al. (1996).*

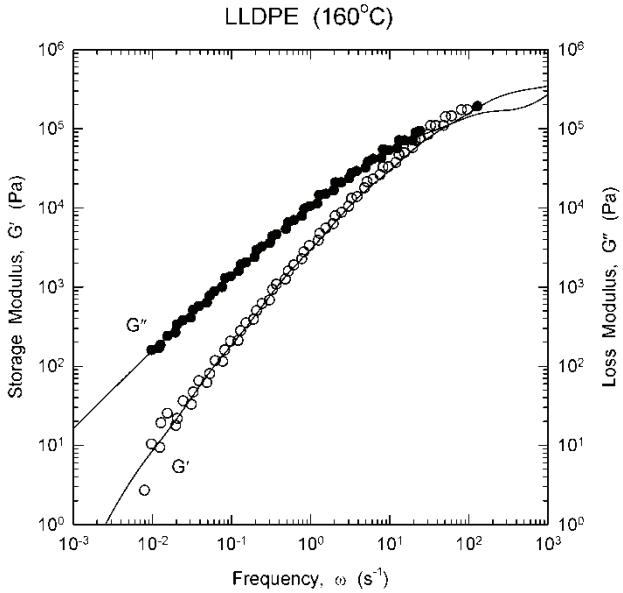

Fig. 3. *Model predictions of storage modulus G' and loss modulus G'' vs. frequency ω for the LLDPE melt at 160°C using Eq. (5) with the material parameters given in Table 1. Symbols are experimental data reported by Guillet et al. (1996).*

4. METHOD OF SOLUTION

The above momentum conservation equation, Eq. (4), is solved using the finite element method with unknown the axial velocity v_z. The viscoelastic stresses are split into a viscous component with a reference viscosity to derive a diffusive term in the momentum equation and into an elastic term, which enters the calculations as a pseudo-body force, as

explained in detail by Luo & Tanner (1986). Galerkin discretization is maintained and the numerical algorithm for convergence is Picard iteration.

The constitutive equation is solved together with the conservation equation using a 15-point Gauss-Laguerre quadrature suited for exponentially fading functions as done in previous simulations for integral models (Luo & Mitsoulis, 1990a,b). As mentioned earlier, particle tracking is simplified and only required in the *z*-direction for rectilinear axial flows. Also essential for a smooth solution is the Galerkin averaging of the velocity gradients, as was done by Luo & Mitsoulis (1990a,b).

In the numerical simulations, two strategies may be followed:

- either the pressure drop is set and the flow rate is calculated from the converged velocity field according to Eq. (3),
- or the flow rate is set and the pressure drop has to be found iteratively using Newton's method.

The latter strategy is chosen, which involves the solution of the FEM equations for every pressure-drop guess. This approach has been used here since the flow rates are those used by Normandin et al. (1999) in their three-dimensional simulation study of LLDPE extrusion, namely $\dot{m} = 30, 200, 385, 407$ g/hr.

5. RESULTS AND DISCUSSION

Newtonian fluids

Newtonian fluids are studied for the different geometries under consideration. The rectangular flow domains under study are symmetric in x and y, and therefore only one quadrant is necessary for the calculations. The annular flow domains are symmetric only in y, thus necessitating half the domain for the calculations. In each case, the computational domains were discretized into 400 (20x20 or 10x40) biquadratic Lagrangian elements. The corresponding values for the geometric parameters used in the simulations are given in Table 2. Typical finite element grids are shown in figure 4. It should be noted that all results were first obtained with coarse 10x10 grids, giving 100 elements. The preliminary runs with the coarse grids were used to gain experience with the solution process. Then the final runs were made with the fine 400-element grids. The results were visually identical, and small numerical differences in the order of 10^{-2} were noted. This is not surprising because the geometries involved here are smooth without singularities, and the problems at hand are easier to solve than the previous 2-D ones involving contractions and exit flows from dies (Luo & Mitsoulis, 1990a,b).

Table 2. *Geometry data for the case of square and concave rectangular, and eccentric annular ducts*

Ducts	H	W	A	R_h
s1x1	1	1	1	0.25
c1x1	1	1	0.73332	0.178674

Annuli	R_i	R_o	d*	e*	e	δ	A	R_h
A4	0.5	1	0.5	0.375	0.75	1.0	2.356194	0.25

s = straight, c = concave, $d^* = R_o - R_i$, $e = e^*/d^*$, $\delta = d^*/R_i$

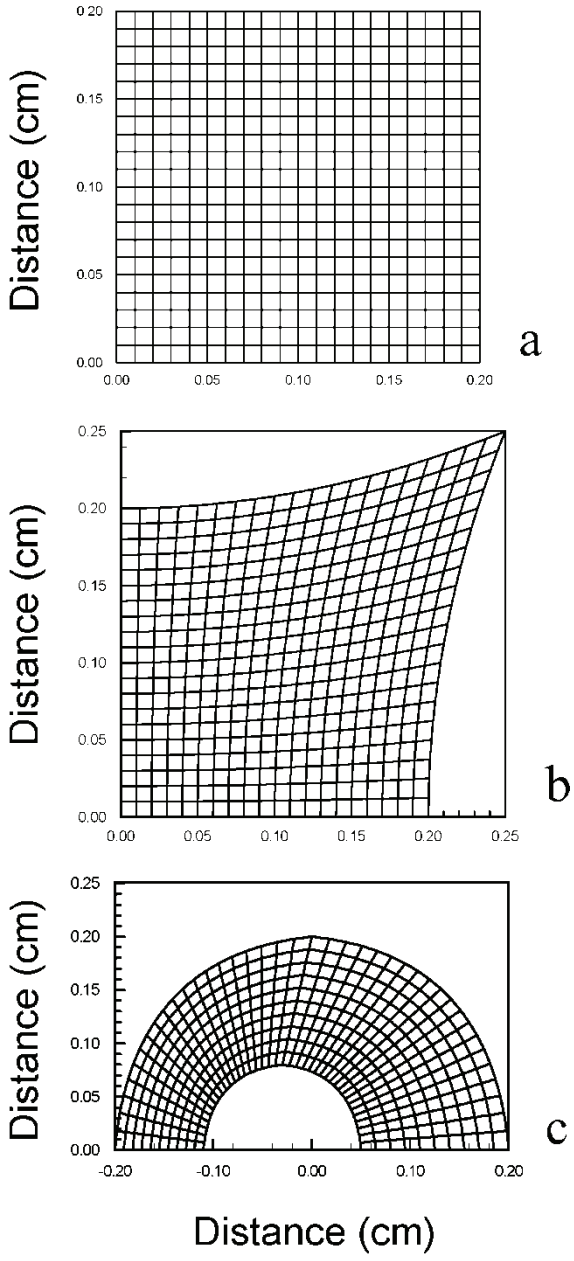

Fig. 4. *Finite element grids used for different duct geometries: (a) square, (b) concave (only ¼ of the domain is shown) (c) eccentric annular (only ½ of the domain is shown).*

As expected from dimensionless analysis, the solution for *dP/dz*, when given as a dimensionless Hagen number, *Ha*, is a unique quantity dependent only on geometry. For the square geometry, we have *Ha*=7.1134, for the concave *Ha*=5.7848, and for the eccentric annulus *Ha*=110.4526. The same values have been found by Pham and Mitsoulis (1998) in the limit of zero Bingham number in their analysis of viscoplastic flows in ducts.

Maxwell fluids

The upper convected Maxwell (UCM) model can be used for reference purposes. The solution process starts from the Newtonian solution and then continuation is used to increase the flow rate (or correspondingly the Weissenberg number, *Ws*). Since the viscosity of the UCM is a constant and through dimensionless arguments, it is expected that the Hagen number, *Ha*, will be the same for all flow rates and the same as the Newtonian one, depending only on geometry. This was borne out from the calculations for all cases examined. However, the stresses are much higher than the Newtonian ones. Also convergence was very slow as the *Ws* number increased. For the highest flow rate value corresponding to a *Ws* = 80.6, the number of iterations needed for the square duct was 3500 starting from the Newtonian solution to satisfy a norm-of-the-error below 10^{-5}.

The results are summarized in Table 3 for the 3 geometries, where it is seen that for all *Ws* numbers the Hagen number is constant for each geometry, as expected.

Table 3. *Dimensionless numbers and pressure drops in flow through ducts of different shapes. Results from the simulations with the UCM integral model*

Square			*Concave*			*Eccentric*		
Ws	$\bar{\dot{\gamma}}$ *(1/s)*	*Ha*	*Ws*	$\bar{\dot{\gamma}}$ *(1/s)*	*Ha*	*Ws*	$\bar{\dot{\gamma}}$ *(1/s)*	*Ha*
5.9	0.57	7.113	5.7	0.55	5.790	15.0	1.45	110.453
39.2	3.78	7.113	38.3	3.69	5.785	100.2	9.65	110.455
75.4	7.27	7.113	73.7	7.10	5.785	192.9	18.57	110.455
79.8	7.68	7.113	77.9	7.50	5.785	203.9	19.63	110.457

LLDPE melt

The LLDPE melt used in the experiments by Normandin et al. (1999) is modelled by the K-BKZ integral constitutive equation with the parameters of Table 1, for the whole range of experimental flow rates (i.e., $\dot{m} = 30, 200, 385, 407$ g/hr). In general, it was much easier to obtain convergence than it was with the Maxwell model. Thus, about 135 iterations were needed to achieve a norm of the error below 10^{-5} for the highest flow rate encountered in the experiments (407 g/hr). The results for the square duct with H = 0.4 cm are given in Table 4. It is seen that the Hagen number is decreasing as the flow rate increases. This is though expected because of the shear thinning character of the polymer melt. The expected pressure drops for a die length of L = 8 cm are also given in the last column. It would be interesting to compare these values with experimental ones in the experiments by Normandin et al. (1999). Unfortunately, pressure values were not given, only the amount of extrudate swell from the experiments.

Table 4. *Dimensionless numbers and pressure drop in flow of an LLDPE melt at 160°C through a square duct with H = 0.40 cm and L = 8 cm. Density ρ = 0.92 g/cm³. Results from the simulations with the K-BKZ model*

$\dot{m}$ *(g/hr)*	*Ws*	$\bar{\dot{\gamma}}$ *(1/s)*	*dP/dz (MPa/cm)*	*Ha*	*ΔP (MPa)*
30	5.9	0.57	0.1108	4.79	0.8864
200	39.2	3.78	0.4719	3.06	3.7752
385	75.4	7.27	0.7270	2.45	5.8160
407	79.8	7.68	0.7527	2.40	6.0216

It is interesting to show the velocity and stress contours for this case. Representing the stresses is the magnitude $|\bar{\tau}|$ of the stress tensor given by

$$|\bar{\tau}| = \sqrt{1/2(\tau/\tau)} \qquad (14)$$

This is done in figure 5, where the values are given in real units for the highest flow rate of 407 g/hr. The minimum value for the velocity is zero and is the boundary contour, while the maximum is at the center of the duct. The minimum value for the magnitude of the stresses is zero and is at the center of the duct, while the maximum is at the center-wall. Similar contours are given for the other two geometries, i.e. for the concave duct in figure 6 and for the eccentric annulus in figure7. It should be noted that the contour shapes are the same for all flow rates, but the values change.

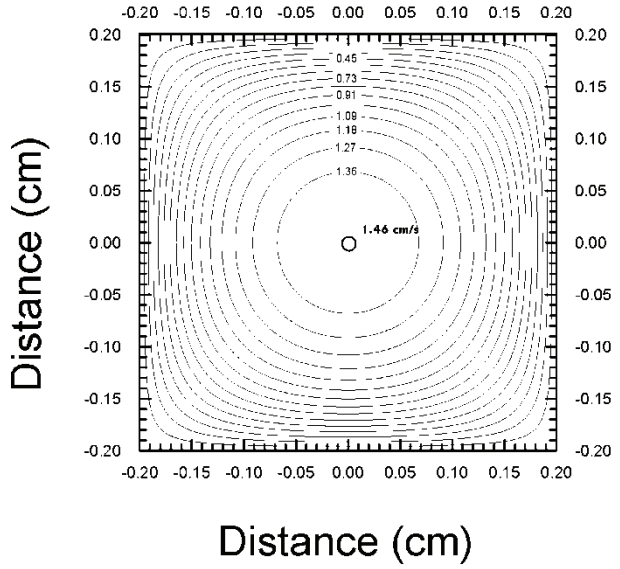

Fig. 5. Velocity contours (upper half) and contours of the magnitude of the stress tensor (lower half) for the highest flow rate (407 g/hr) in flow of an LLDPE melt through the square duct used in the experiments by Normandin et al. (1999). The maxima are shown with a open circle.

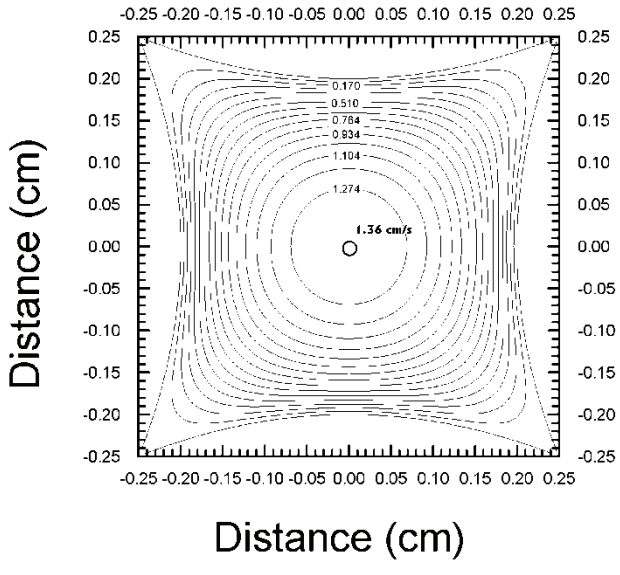

Fig. 6. Velocity contours (upper half) and contours of the magnitude of the stress tensor (lower half) for the highest flow rate (407 g/hr) in flow of an LLDPE melt through a concave duct. The maxima are shown with a open circle.

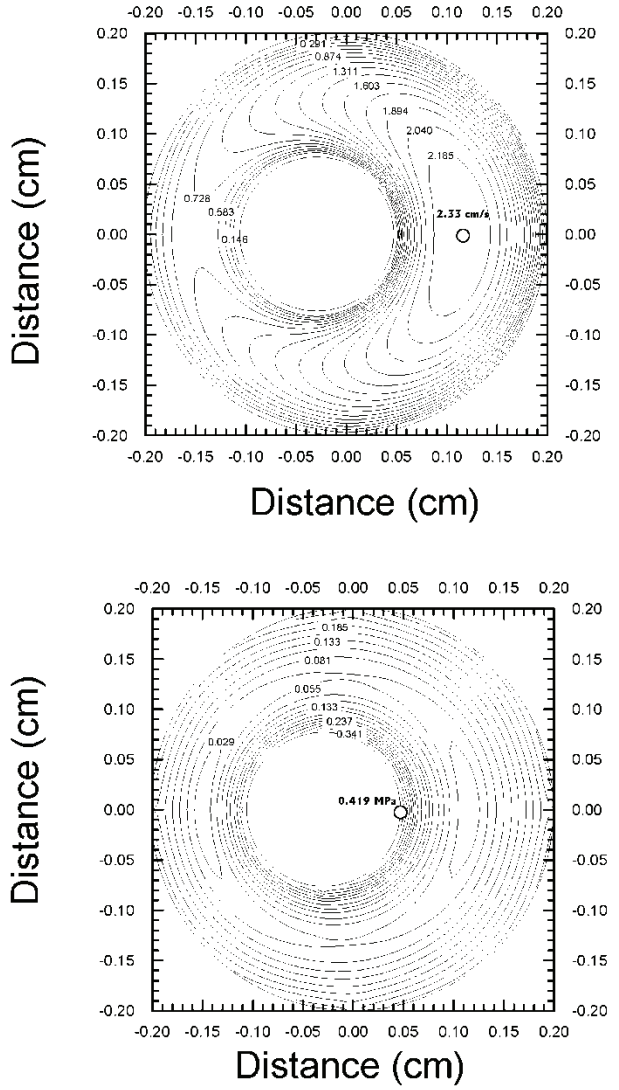

Fig. 7. *Velocity contours (upper half) and contours of the magnitude of the stress tensor (lower half) for the highest flow rate (407 g/hr) in flow of an LLDPE melt through an eccentric annulus. The maxima are shown with a open circle.*

6. SUMMARY

The present results are offered mainly as benchmark solutions for checking purposes for viscoelastic flows of the integral K-BKZ type, including the Maxwell fluid. They can be particularly useful in determining fully developed profiles in ducts, especially for entering the boundary conditions in three-dimensional simulations. The drawback of course is the lack of secondary flows, but then this has been addressed before in the references mentioned above. For cases where the second normal-stress difference is zero or negligible, the present results are valid. They can also be used for design purposes to find out the optimal geometry to achieve a certain flow rate with the minimum pressure drop in the system.

ACKNOWLEDGEMENTS

Financial assistance from NSERC of Canada and the National Technical University of Athens (NTUA) is gratefully acknowledged.

REFERENCES

Debbaut, B., Avalosse, T., Dooley, J., Hughes, K., 1997, On the development of secondary motions in straight channels induced by the second normal stress difference: experiments and simulations, *J. Non-Newtonian Fluid Mech.*, 69, 255-271.

Dupont, S., Crochet, M.J., 1987, Swirling flows of viscoelastic fluids of the integral type in rheogoniometers, *Chem. Eng. Comm.*, 53, 199-221.

Guillet, J., Revenu, P., Béreaux, Y., Clermont, J.-R., 1996, Experimental and numerical study of entry flow of polyethylene melts, *Rheol. Acta*, 35, 494-507.

Gervang, B., Larsen, P.S., 1991, Secondary flows in straight ducts of rectangular cross section, *J. Non-Newtonian Fluid Mech.*, 39, 217-237.

Huilgol, R.R., Panizza, M.P., 1995, On the determination of the plug flow region in Bingham fluids through the application of variational inequalities, *J. Non-Newtonian Fluid Mech.*, 58, 207-217.

Luo, X.-L., Mitsoulis, E., 1990a, An efficient algorithm for strain history tracking in finite element computations of non-Newtonian fluids with integral constitutive equations, *Int. J. Num. Meth. Fluids*, 11, 1015-1031.

Luo, X.-L., Mitsoulis, E., 1990b, A numerical study of the effect of elongational viscosity on vortex growth in contraction flows of polyethylene melts, *J. Rheol.*, 34, 309-342.

Luo, X.-L., Tanner, R.I., 1986, A streamline element scheme for solving viscoelastic flow problems, Part II. Integral constitutive models, *J. Non-Newtonian Fluid Mech.*, 22, 61-89.

Luo, X.-L., Tanner, R.I., 1988, Finite element simulation of long and short circular die extrusion experiments using integral models, *Int. J. Num. Meth. Eng.*, 25, 9-22.

Middleman, S., 1965, Flow of power-law fluids in rectangular ducts, *Trans. Soc. Rheol.,* 9, 83-95.

Normandin, M., Clermont, J.-R., Guillet, J., Raveyré, C., 1999, Three-dimensional extrudate swell: experimental and numerical study of a polyethylene melt obeying a memory integral equation, *J. Non-Newtonian Fluid Mech.*, 87, 1-25.

Papanastasiou, A.C., Scriven, L.E., Macosko, C.W., 1983, An integral constitutive equation for mixed flows: viscoelastic characterization, *J. Rheol.*, 27, 387-410.

Pham, T.V., Mitsoulis, E., 1998, Viscoplastic flows in ducts, *Can. J. Chem. Eng.*, 76, 120-125.

Tanner, R.I., 2000, *Engineering rheology*, 2nd edn., Clarendon Press, Oxford.

Taylor, A.J., Wilson, S.D.R., 1997, Conduit flow of an incompressible, yield-stress fluid, *J. Rheol.*, 41, 93-101.

Wachs, A., Clermont, J.R., Normandin, M., 1999, Fully-developed flow and temperature calculations for rheologically complex materials using a mapped circular domain, *Eng. Comp.*, 16, 807-830.

Walton, I.C., Bittleston, S.H., 1991, The axial flow of a Bingham plastic in a narrow eccentric annulus, *J. Fluid Mech.*, 222, 39-60.

Xue, S.C., Phan-Thien, N., Tanner, R.I., 1995, Numerical study of secondary flows of viscoelastic fluid in straight pipes by an implicit finite volume method, *J. Non-Newtonian Fluid Mech.*, 59, 191-213.

PROSTOLINIOWY LEPKOPLASTYCZNY PRZEPŁYW PRZEZ KANAŁ

Streszczenie

W pracy opisano badania osiowego przepływu przez kanał dla lepkoplastycznego materiałów, w tym dla liniowego polietylenu o niskiej gęstości. Lepkoplastyczność jest opisana przez całkowe równanie konstytutywne typu K-BKZ ze spektrum czasów relaksacji, które dopasowano do wyników badań doświadczalnych dla lepkości na ścinanie i wydłużenie i dla normalnych naprężeń zmierzonych w przepływie ze ścinaniem. Model K-BKZ może zostać zredukowany do modelu Newtona i Maxwella poprzez odpowiedni dobór współczynników. W ramach projektu opracowano nową technikę, w której tensory Fingera i Cauchy'ego-Greena są uproszczone do przepływów osiowych, ponieważ śledzenie ruchu cząstki jest wymagana tylko w jednym kierunku z (nie ma potrzeby śledzenia ruch w płaszczyźnie x, y). W pracy przedstawiono rozwiązanie numeryczne dla dwuwymiarowych obszarów na przekroju poprzecznym. Rozważono przekroje kwadratowy, wklęsły kwadratowy i ekscentryczny dla różnych prędkości przepływu i różnych spadków ciśnienia. Dla modelu Maxwella bezwymiarowy spadek ciśnienia jest niezależny od liczby Weissenberga i jest funkcją tylko kształtu obszaru. Dla modelu K-BKZ reprezentującego liniowy polietylen o niskiej gęstości, spadek bezwymiarowego ciśnienia zmniejsza się ze wzrostem prędkości przepływu, a zatem także ze wzrostem liczby Weissenberga. Przedstawione w pracy wyniki są proponowane jako „benchmark" dla nakładania wejściowej prędkości i profilu naprężeń w trójwymiarowych kanałach, kiedy wtórny przepływ nie występuje.

Submitted: April 22, 2008
Submitted in a revised version: June 6, 2008
Accepted: July 7, 2008